

1 **Applying landscape metrics to species distribution model predictions to characterise**
2 **internal range structure and associated changes**

3

4 **Running Title:** “Better species range characterisation”

5

6 Amelia Curd^{1✉*}, Mathieu Chevalier^{1*}, Mickaël Vasquez¹, Aurélien Boyé¹, Louise B. Firth²,
7 Martin P. Marzloff¹, Lucy M. Bricheno³, Michael T. Burrows⁴, Laura E. Bush⁵, Céline
8 Cordier¹, Andrew J. Davies^{6,7}, J. A. Mattias Green⁸, Stephen J. Hawkins^{2,9,10}, Fernando P.
9 Lima^{11,12}, Claudia Meneghesso^{11,12,13}, Nova Mieszkowska^{10,14}, Rui Seabra¹¹ and Stanislas F.
10 Dubois¹

11

12 ¹ IFREMER, Centre de Bretagne, DYNECO LEBCO, 29280 Plouzané, France.

13 ² School of Biological and Marine Sciences, University of Plymouth, Drake Circus,
14 Plymouth, PL4 8AA, United Kingdom.

15 ³ National Oceanography Centre, Joseph Proudman Building, 6 Brownlow Street, Liverpool,
16 L3 5DA, UK.

17 ⁴ Scottish Association for Marine Science, Scottish Marine Institute, Oban, PA37 1QA, UK.

18 ⁵ FUGRO GB Marine Limited, Gait 8, Research Park South, Heriot-Watt University,
19 Edinburgh EH14 4AP, UK.

20 ⁶ Department of Biological Sciences, University of Rhode Island, Kingston, RI 02881, USA.

21 ⁷ Graduate School of Oceanography, University of Rhode Island, Narragansett, RI 02882,
22 USA.

23 ⁸ School of Ocean Sciences, Bangor University, Askew Street, Menai Bridge, LL59 5AB
24 Bangor, United Kingdom.

25 ⁹ Ocean and Earth Science, University of Southampton, National Oceanography Centre
26 Southampton, Waterfront Campus, European Way, Southampton SO14 3ZH, UK

27 ¹⁰ The Marine Biological Association of the UK, Citadel Hill, Plymouth, PL1 2PB, UK

28 ¹¹ CIBIO, Centro de Investigação em Biodiversidade e Recursos Genéticos, InBIO
29 Laboratório Associado, Campus de Vairão, Rua Padre Armando Quintas, nº 7, 4485-661
30 Vairão, Portugal

31 ¹² BIOPOLIS Program in Genomics, Biodiversity and Land Planning, Campus de Vairão, Rua
32 Padre Armando Quintas, nº 7, 4485-661 Vairão, Portugal

33 ¹³ Departamento de Biologia, Faculdade de Ciências da Universidade do Porto, R. Campo
34 Alegre, s/n, 4169-007 Porto, Portugal

35 ¹⁴ Department of Earth, Ocean and Ecological Sciences, School of Environmental Sciences,
36 University of Liverpool, Nicholson Building, Brownlow Street, Liverpool, L69 3GP, UK

37

38 *Amelia Curd and Mathieu Chevalier should be considered joint first author

39 ✉ E-mail: amelia.curd@ifremer.fr

40

41 **Abstract**

42 Distributional shifts in species ranges provide critical evidence of ecological responses to
43 climate change. Assessments of climate-driven changes typically focus on broad-scale range
44 shifts (e.g. poleward or upward), with ecological consequences at regional and local scales
45 commonly overlooked. While these changes are informative for species presenting continuous
46 geographic ranges, many species have discontinuous distributions - both natural (e.g.
47 mountain or coastal species) or human-induced (e.g. species inhabiting fragmented
48 landscapes) - where within-range changes can be significant. Here, we use an ecosystem
49 engineer species (*Sabellaria alveolata*) with a naturally fragmented distribution as a case

50 study to assess climate-driven changes in within-range occupancy across its entire global
51 distribution. To this end, we applied landscape ecology metrics to outputs from species
52 distribution modelling (SDM) in a novel unified framework. SDM predicted a 27.5% overall
53 increase in the area of potentially suitable habitat under RCP 4.5 by 2050, which taken in
54 isolation would have led to classify the species as a climate change winner. SDM further
55 revealed that the latitudinal range is predicted to shrink because of decreased habitat
56 suitability in the equatorward part of the range, not compensated by a poleward expansion.
57 The use of landscape ecology metrics provided additional insights by identifying regions that
58 are predicted to become increasingly fragmented in the future, potentially increasing
59 extirpation risk by jeopardising metapopulation dynamics. This increased range fragmentation
60 could have dramatic consequences for ecosystem structure and functioning. Importantly, the
61 proposed framework - which brings together SDM and landscape metrics - can be widely
62 used to study currently overlooked climate-driven changes in species internal range structure,
63 without requiring detailed empirical knowledge of the modelled species. This approach
64 represents an important advancement beyond predictive envelope approaches and could
65 reveal itself as paramount for managers whose spatial scale of action usually ranges from
66 local to regional.

67

68

69 **Keywords (6-10 words or phrases)**

70 Climate change | Range fragmentation | Engineer species | Species distribution modelling |

71 Landscape metrics | Within-range structure | Patch dynamics

72

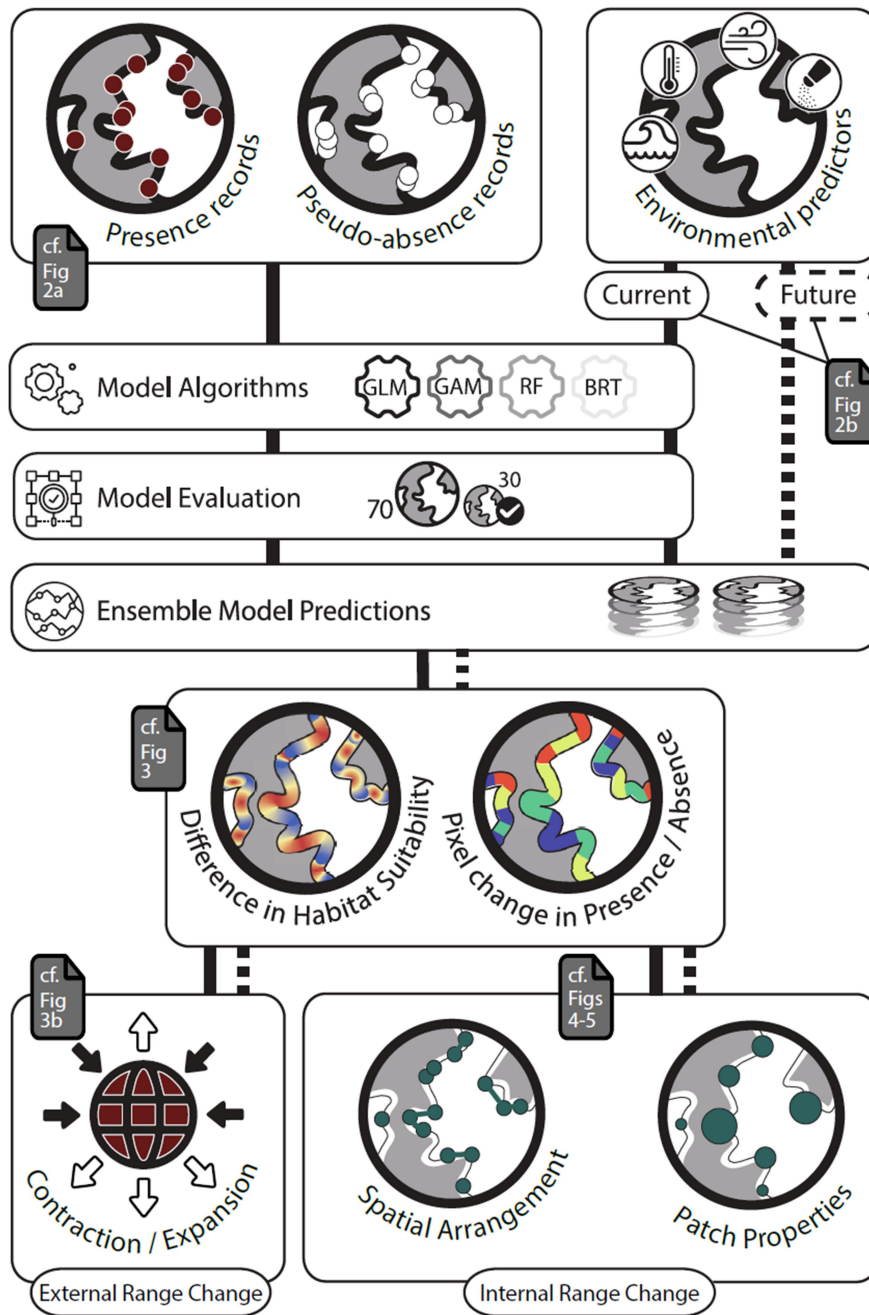
73

74

75 | INTRODUCTION

76 Geographic distributions of species are determined by complex interactions and feedbacks
77 between climate, ecological and evolutionary processes (Parmesan and Yohe, 2003; Burrows
78 et al., 2020; Paquette and Hargreaves, 2021). Several pioneering studies have shown the
79 profound implications of climate-driven modification on assemblage composition, community
80 structure and ecosystem functioning (Pecl et al., 2017; Walther, 2010). Under future climate
81 conditions, the geographic ranges of many species are predicted to shift in size, latitude, depth
82 and/or elevation (Poloczanska et al., 2016; Pinsky et al., 2020). Such changes have typically
83 been documented for either the leading poleward or trailing equatorward range edges (i.e. the
84 external range structure), thus overlooking changes taking place within ranges (i.e. the
85 internal range structure; Csergő et al., 2020).

86



87

88 **FIGURE 1. Modelling framework bringing together SDM outputs and landscape**
 89 **metrics.** SDMs were fitted on spatially thinned presence records and randomly-generated
 90 pseudo-absences (see Figure 2a). Six environmental predictors: minimum air temperature,
 91 maximum sea surface temperature, fetch, salinity, wave height and tidal amplitude (see Figure
 92 2b) were used to explain the species spatial distribution. Four algorithms were selected to
 93 build the models: GLM (generalized linear models), GAM (generalized additive models), RF
 94 (random forests) and BRT (boosted regression trees). We used an ensemble model approach

95 to predict and map the current and the future habitat suitability across the species latitudinal
96 range. Habitat suitability is defined as the likelihood of occurrence of a species in association
97 with environmental variables. Ensemble predictions were then binarised into
98 presence/absence (P/A) maps. These P/A maps were then used to (1) evaluate changes in
99 range size and distribution shifts (see Figure 3b) and (2) compute various landscape metrics
100 using both current and future P/A predictions. The landscape metrics were then used to study
101 the spatial arrangement of predicted patches of P/A within the species range over time
102 (Figures 4-5). Note that we applied landscape metrics to outputs from the ensemble model,
103 however this approach can be applied separately to each model output in order to obtain
104 information regarding the influence of pseudo-absence datasets, model runs and algorithms on
105 internal range change metrics.

106

107 Perhaps this omission betrays the implicit assumption that species distributions are spatially
108 continuous (e.g. most IUCN polygons are continuous; Rocchini et al., 2011). Under this
109 supposition, focusing on measuring changes in the external range structure such as changes in
110 range size (Pither, 2003; Thomas, 2012), or quantifying the velocity at which the range
111 centroid and/or margins (trailing and leading edges) may shift in the future may suffice
112 (Sunday et al., 2012; Lenoir et al., 2020; Fredston-Hermann et al., 2020). However, by relying
113 only on external metrics, these broad-scale studies overlook the changes that can take place
114 within ranges and which ultimately determine the abundance, occurrence and connectivity of
115 local populations (VanDerWal et al., 2013). For instance, regional persistence of rare species,
116 or those living in fragmented landscapes such as mountainous, coastal or degraded areas,
117 usually present discontinuous distributions that rely on complex networks of interconnected
118 populations whose responses to climate-driven changes cannot be accurately assessed using
119 metrics characterising broad-scale patterns in biogeographical distribution changes (Opdam &
120 Wascher, 2004; Mestre et al., 2017). In such cases, quantifying changes in the internal
121 structure of geographical ranges is critical for understanding species vulnerability to climate
122 change. For instance, range fragmentation can increase local extinction risk by jeopardising

123 metapopulation dynamics (Mestre et al., 2017). To illustrate this point, we focused on the
124 naturally discontinuous distribution of an intertidal ecosystem engineer, the reef-building
125 honeycomb worm *Sabellaria alveolata* (Linnaeus, 1767).

126 Intertidal ecosystems - and engineered intertidal habitats in particular - support high
127 biodiversity and deliver important ecosystem services to society such as protection from
128 erosion and flooding, water quality, food resources (shellfish, seaweeds), sites for aquaculture
129 and fish nursery grounds (Barbier et al., 2011). These ecosystems are however facing strong
130 pressures, being under the influence of multiple stressors acting at multiple scales (regional
131 and local) whose effect on biodiversity can be reinforced by climate change (Bugnot et al.,
132 2021). Moreover, intertidal species are exposed to both terrestrial and marine environmental
133 conditions, which remain challenging to account for (Helmuth et al., 2006). Taking advantage
134 of extensive occurrence records (Curd et al., 2020), coupled with fit-for-purpose resolution
135 (0.083 decimal degrees,) current and future climatologies of marine and terrestrial conditions,
136 we developed a species distribution model (SDM) to predict the current and future
137 distribution of *S. alveolata* across its full global latitudinal range (32-61° N). We then
138 assessed how the external and internal range structure of *S. alveolata* will be altered in
139 response to climate change. The latter was assessed by making novel use of landscape metrics
140 applied to SDM outputs.

141 Landscape ecology is a discipline all unto itself (Turner et al. 2005). A great variety of
142 landscape composition (e.g., the number and amount of different habitat types) and
143 configuration (the spatial arrangement of those classes) metrics have been developed for
144 categorical data (Lausch et al., 2015). These metrics make it possible to improve our
145 understanding of, for example, the effect of landscape complexity on biodiversity (Schindler
146 et al., 2013) or habitat connectivity on metapopulation dynamics (Howell et al., 2018). The
147 cornerstone of our approach is to have transformed species' predicted presence and absence

148 into binary patches, where each patch is composed of one or several adjacent pixels of the
149 same type (e.g. presences). This biotic-centred approach contrasts with the classical
150 application of landscape metrics where patches are often derived from land-cover maps
151 (Uuemaa et al., 2013). Once patches of predicted presences and absences are identified,
152 various landscape metrics can be used to characterise patch properties and their spatial
153 structure, ultimately providing a better characterization of the internal range structure and how
154 it will evolve in response to external pressures (e.g. climate change).

155

156 **2 | MATERIALS AND METHODS**

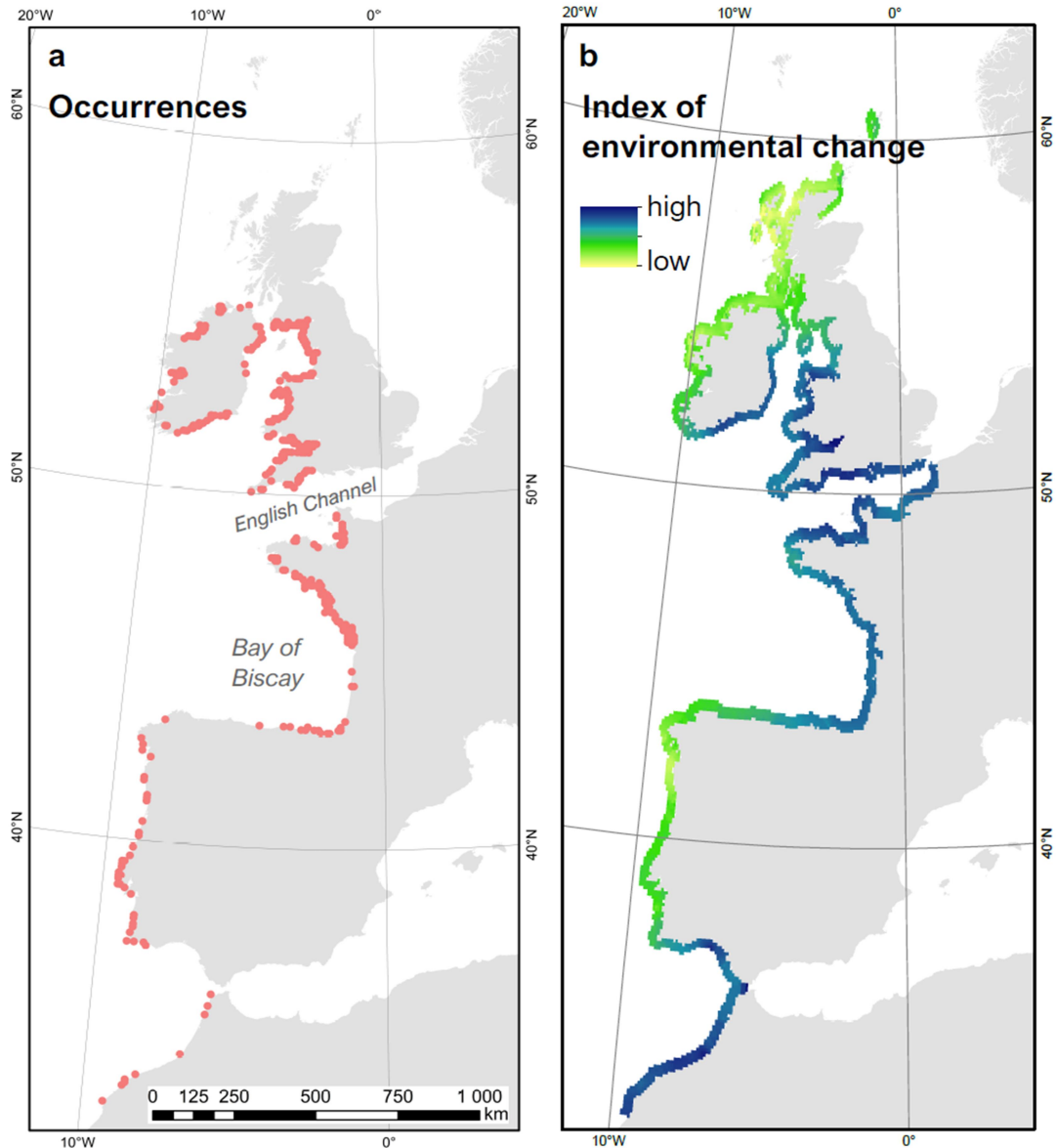
157 Our workflow, which combines landscape ecology metrics with species distribution model
158 outputs is illustrated in Figure 1.

159

160 **2.1 | Study area and species**

161 The honeycomb worm *Sabellaria alveolata* is an intertidal ecosystem engineer, capable of
162 building tubes from sand and shell fragments on low- to mid-shore, in semi-exposed and
163 exposed locations. As a colonial species, the multitude of fused tubes form biogenic structures
164 ranging from veneers and hummocks to large reefs (Wilson, 1971; Curd et al., 2019). Reef-
165 forming *S. alveolata* has the potential to provide important coastal protection (Naylor & Viles,
166 2000) and biogenic habitat for a diverse range of other species (Dubois et al., 2002; Jones et
167 al., 2018). *Sabellaria alveolata* has a discontinuous distribution ranging from southern
168 Morocco to southwest Scotland (Lourenço et al., 2020), with many distribution breaks (Firth
169 et al., 2021a) (Figure 2a).

170



171

172 **FIGURE 2. Species occurrence records and index of environmental change along the**
 173 **species distributional range. a,** The 363 thinned occurrence records collated between 2000-
 174 2019 from multiple data sources highlight the broad but fragmented biogeographical range of
 175 *S. alveolata*. **b,** Index of change in local environmental conditions (Table S1) between current
 176 and future (RCP 4.5 in 2050) climatic layers. High values indicate the largest difference
 177 between current and future environmental conditions (for details regarding the index
 178 computation, see the Methods).

179

180 Our study was conducted across 29 degrees of latitude (from 32°N to 61°N) spanning a large
181 gradient of climatic conditions (Figure S1). To the best of our knowledge *S. alveolata* is, and
182 has always been, absent from the North Sea (Nunes et al., 2021). Although it has occasionally
183 been cited as present in the North Sea (Richter, 1927), expert consensus is that these
184 occurrences were *S. spinulosa* reefs (Reise, pers. comm.) (Figure S2). This distribution limit
185 is thought to be due to the presence of a long-term hydrographic barrier to larval dispersal at
186 the Cherbourg Peninsula in the English Channel (Salomon & Breton, 1993), and to
187 competitive exclusion by *S. spinulosa* in the Greater North Sea. As both larval dispersal and
188 biotic interactions cannot be accounted for by SDM, our study area does not extend to the
189 North Sea. Since we only consider intertidal *S. alveolata* bioconstructions, our study area does
190 not extend to the Mediterranean, where all *S. alveolata* records are subtidal owing to low
191 amplitude tides.

192

193 **2.1 | Occurrence records**

194 An increasing number of SDM studies are based on presence data downloaded from the
195 Global Biodiversity Information Facility (GBIF) (Alhajeri & Fourcade, 2019). Although these
196 data have proved useful to model the distribution of some well-known species, records for *S.*
197 *alveolata* are strongly affected by spatial sampling bias (Firth et al., 2021b) (Figure 2a). Here,
198 we collated occurrence records from numerous sources, including field observations, research
199 articles, citizen science observations, management reports and online databases (Curd et al.,
200 2020). Presence records were considered between the years 2000-2019, a time span
201 compatible with the temporal coverage of climatic layers classically used in SDM studies (e.g.
202 Bio-ORACLE, Worldclim) (Assis et al., 2018; Hijmans et al., 2005; Tyberghein et al., 2012).
203 Subtidal observations, and observations without geographic accuracy down to shore level,
204 were excluded. Overall, 98 literature sources were included in the analysis, resulting in 14,960

205 occurrence records. Only 12.2% of these records were previously accessible via online
206 databases (Curd et al., 2020). Occurrence records were spatially thinned so that only one
207 record was retained per climatic-grid cell (Steen et al., 2021). This left us with 363
208 observations.

209

210 **2.3 | Environmental variables**

211 We retained only ‘scenopoetic’ variables (i.e. variables on which the species has no impact)
212 as predictors (Hutchinson, 1978). We did not include available seabed substrate maps
213 (although potentially relevant) because the best existing layer compilation (currently provided
214 by EMODnet; <https://emodnet.ec.europa.eu/en>) was not deemed fit-for-purpose, due to low
215 spatial accuracy in many areas and limited spatial coverage. All environmental predictors
216 covered the full latitudinal distribution of *S. alveolata* and came at a spatial resolution of
217 0.083° decimal degrees, which corresponds to a distance of 9.3 km along the latitude axis and,
218 along the longitude axis, 7.8 km at the equatorward edge of the study area and 4.5 km at the
219 poleward edge. Specifically, a set of 10 bioclimatic variables were chosen as climate-related
220 candidate predictors (Table S1) including air temperature (min, max and mean) from
221 WorldClim version 1.4 (Hijmans et al., 2005), sea-surface temperature (min, max and mean)
222 and mean salinity from Bio-ORACLE (Assis et al., 2018; Tyberghein et al., 2012), wave
223 height (Bricheno & Wolf, 2018), wave fetch (i.e. the distance over which wind-driven waves
224 can build given the orientation of the coastline, Burrows, 2020) and tidal current and surface
225 amplitudes from the TPXO8 ATLAS solution (www.tpxo.net) (Egbert & Erofeeva, 2002;
226 Egbert et al., 2010). Present and future wave height was estimated by applying the
227 WaveWatch IIITM spectral wave model at a regional scale (Atlantic Europe) (Tolman, 2009).
228 Because wave fetch was estimated at a 100 m resolution, we re-projected and upscaled this

229 raster (using average values) to match with the resolution of the other rasters (i.e. 0.083°
230 degrees).

231 We checked for collinearity between variables using Pearson's correlation coefficients. For
232 pairs with Pearson's $|r| > 0.7$, we retained the variable known to be the most ecologically
233 relevant (Araújo et al., 2019). This process led us to select six predictors: maximum sea-
234 surface temperature, average salinity, minimum air temperature, wave fetch, wave height and
235 tidal amplitude (Figures S3-S7).

236 Future predictions for four of the six selected predictors were obtained for horizon 2050 under
237 the Representative Concentration Pathway scenario RCP 4.5 (Meinshausen et al., 2011):
238 salinity and sea surface temperature from Bio-ORACLE, air temperature from WorldClim
239 and wave height from Bricheno & Wolf (2018). Tidal amplitude and wave fetch were
240 assumed to stay constant in the future. To evaluate where, over the range, climate change
241 might have the strongest effect on *S. alveolata* reefs, we calculated an index of environmental
242 change. For this purpose, we first computed a climatic space using a principal component
243 analysis (PCA) performed on the four standardised environmental variables that are predicted
244 to change in the future (Figure S8). Then, we projected future environmental values within the
245 two-dimensional space defined by the two first PCA axes (explaining 82% of the variance).
246 Hence, a given pixel has two positions in this space. The index was calculated as the
247 Euclidean distance between present and future conditions for each pixel (Figure 2b) with
248 greater distances indicating larger changes.

249

250 **2.4 | Model building**

251 Model building was performed in R (R Core Team, 2019) using the package 'biomod2'
252 (Thuiller et al., 2009). Four fundamentally different algorithms were selected to build the

253 SDMs: generalised linear models (McCullagh & Nelder, 1998), generalised additive models
254 (Hastie & Tibshirani, 1986), random forests (Breiman, 2001), and boosted regression trees
255 (Elith et al., 2008). The four algorithms have already proven useful in modelling benthic
256 species distributions (Bučas et al., 2013) and were selected for their ability to model non-
257 linear relationships while assuming different shapes for the response curves. These algorithms
258 have their own set of strengths and weaknesses which can lead to contrasted predictions (de la
259 Hoz et al., 2019). For instance, random forests generally display high predictive performance
260 on the training dataset (Elith, 2006; Reiss et al., 2011) but are prone to overfitting which can
261 yield inaccurate predictions when extrapolating to non-analog conditions (Wenger & Olden,
262 2012; Beaumont et al., 2016). Alternatively, GLMs often have a lower predictive accuracy on
263 the training dataset but usually display higher transferability (Wenger & Olden, 2012;
264 Heikkinen et al., 2012; Yates et al., 2018). Algorithms were fitted using the default settings of
265 biomod2.

266 The four approaches require presence-absence data to be fitted. Since the absence records in
267 our database had an uneven spatiotemporal spread (see Figure S1), we generated a random set
268 of pseudo-absences over the study area. We generated the same number of pseudo-absences
269 as available presences (i.e. 363) to give an equal weight to presences and absences in model
270 predictions (Barbet-Massin et al., 2012). Models were then fitted on this presence/pseudo-
271 absence dataset. To account for stochasticity regarding the selection of pseudo-absences, this
272 procedure was repeated 10 times (i.e. ten pseudo-absence datasets were generated). Note that
273 since we used pseudo-absences, the models predict a habitat suitability index ranging from 0
274 to 1 rather than a probability of presence (Guisan et al., 2017) (Figure S9).

275

276

277

278 **2.5 | Model performance and ensemble predictions**

279 Models were evaluated using a cross-validation approach based on repeated split-sampling
280 (70% for calibration, 30% for evaluation) with 10 runs (Figure 1). For each run (and each
281 pseudo-absence dataset), model performance was assessed using the true skill statistic (TSS)
282 (Allouche et al., 2006) and the area under the ROC curve (AUC; Hanley and McNeil 1982).
283 Both TSS (Sensitivity + Specificity - 1) and AUC are prevalence (i.e. the ratio of ‘presence’
284 to ‘absence’ in the dataset) independent. They provide information on the model’s capacity to
285 distinguish between presence and absence classes, with higher values pointing to better
286 models (Lawson et al., 2014). Overall, a total of 400 models (4 algorithms times 10 cross-
287 validations times 10 pseudo-absence samplings) were fitted. The importance of the different
288 predictors across datasets and algorithms was evaluated using the “variables_importance”
289 function of biomod2.

290 We used an ensemble modelling approach to perform current and future predictions over the
291 distribution range (Hao et al., 2020). Only models whose predictions on the test data had a
292 $TSS \geq 0.5$ were retained for this procedure (99 GAM + 89 GLM + 100 RF + 99 BRT).
293 Current and future predictions from the 387 contributing models were combined using a
294 weighted average based on TSS scores (i.e. higher influence of models or datasets with higher
295 TSS). Present and future predictive ensemble maps were reclassified into binary presence-
296 absence surfaces using the threshold that maximises TSS evaluation scores (i.e. maxTSS;
297 Guisan et al., 2017).

298

299 **2.6 | Measuring broad-scale external range changes between periods**

300 Binary predictions are classically used to estimate how species ranges will be affected in the
301 future (Yalcin & Leroux, 2017). While the main object of inference focuses on range size

302 (Gaston, 1996), additional metrics can be found in the literature (e.g. the proportion of pixels
303 lost or gained) (Thuiller, 2004). When considering a broad latitudinal gradient, a more
304 accurate estimation of changes in range size can be obtained by giving an equal area to all
305 pixels (Sillero & Barbosa, 2021). Here, we re-projected the predicted rasters (both for
306 presence-absence and habitat suitability) with the ETRS89 Lambert Azimuthal Equal Area
307 Coordinate Reference System (ETRS-LAEA), with the latitude and the longitude of origin
308 adjusted to 44.3°N, -3.2°E, giving each pixel an area of 25 km² (5 km x 5 km). From the
309 presence-absence rasters, we used the BIOMOD_RangeSize function to estimate the
310 proportion and relative number of pixels lost, gained and stable. We also quantified range
311 shifts, another measure frequently used to estimate the effect of climate change on species
312 distribution (e.g. Lenoir et al., 2020). To measure this, we first characterised ranges in both
313 periods considering the centre (median latitudinal value where the species was predicted to be
314 present), the upper (97.5% percentile) and the lower (2.5% percentile) limits of the range. We
315 then quantified range shifts for all three attributes as the difference between future and current
316 values.

317

318 **2.7 | Measuring fine-scale internal range changes between periods**

319 In addition to broad-scale range metrics that describe external range changes, we used
320 landscape metrics to better characterise the fine-scale internal structure of the species range
321 (in both current and future climatic conditions) and provide additional insights regarding how
322 this structure will be affected in the future. Landscape ecologists often conceptualise the
323 landscape as a mosaic of discrete, ecologically homogeneous, patches embedded within a
324 background matrix of inhabitable areas (Turner et al. 2005, Lausch et al. 2015). Patches are
325 the basic statistical unit under this approach, and are defined as one isolated, or several
326 adjacent, pixels of the same class (e.g. crops) that differ from their surroundings (e.g. forests).

327 Each patch has its own individual characteristics (e.g. shape, size, distance to nearest
328 neighbour; Hesselbarth et al. 2019), while the landscape pattern emerges from the spatial
329 composition and configuration of patches from different classes (Turner et al. 2005, Lausch et
330 al. 2015). Pixels belonging to each patch can be monitored over time so that pixels
331 transitioning from one class to another in response to external pressures (e.g. climate change)
332 can be translated into patch dynamics. Thus, presence pixels switching to absence pixels
333 within a presence patch lead to patch fragmentation. A suite of landscape metrics describing
334 changes in patch properties (e.g. area, Euclidean distance to the nearest neighbour), and their
335 spatial configuration (e.g. patch aggregation) can also be used to describe changes at various
336 spatial scales. For instance, an increased distance to the nearest neighbour coupled with a
337 decrease in patch aggregation for presence patches is indicative of population fragmentation.

338 Here, we propose to use landscape metrics on predicted binary (presence and absence) maps
339 obtained from SDMs to simplify, often complex, spatial predictions into a mosaic of discrete
340 patches of predicted presences and absences under both current and future environmental
341 conditions. Landscape metrics can then be used to study presence and absence patch
342 properties and how their spatial arrangement is predicted to change in the future, ultimately
343 providing a better characterization of range changes.

344 Landscape metric analyses were performed using the R package ‘landscapemetrics’
345 (Hesselbarth et al., 2019). This package contains many functions to describe various patch
346 properties (e.g. area, distance to nearest neighbour of the same class). These properties can be
347 aggregated at different spatial scales (e.g. mean patch area at the range scale) and studied over
348 time. Note that the package also provides functions to compute diversity metrics at the
349 landscape scale (i.e. range scale in our case), however since our usage is constrained to binary
350 outputs, most of these functions were not relevant for the purposes of this study. Here, we
351 focused on the patch area for each class, the Euclidean distance to the nearest neighbouring

352 patch of the same class, and the predicted habitat suitability of pixels within patches (a metric
353 that uses an additional level of information derived from SDMs). The latter metric relies on
354 the fact that each pixel contains additional quantitative information (i.e. the habitat suitability
355 values that were used for thresholding which is a necessary step to identify patches) that can
356 be used to better characterise patch properties and their spatial arrangement. Here, we used
357 this information to run a patch-based linear regression to investigate whether average changes
358 in patch suitability (i.e. the average difference between future and current suitability for all
359 pixels within the patch) followed a latitudinal gradient, a classical biogeographical pattern
360 where species are moving poleward to track suitable climatic conditions (Mieszkowska &
361 Sugden, 2016).

362

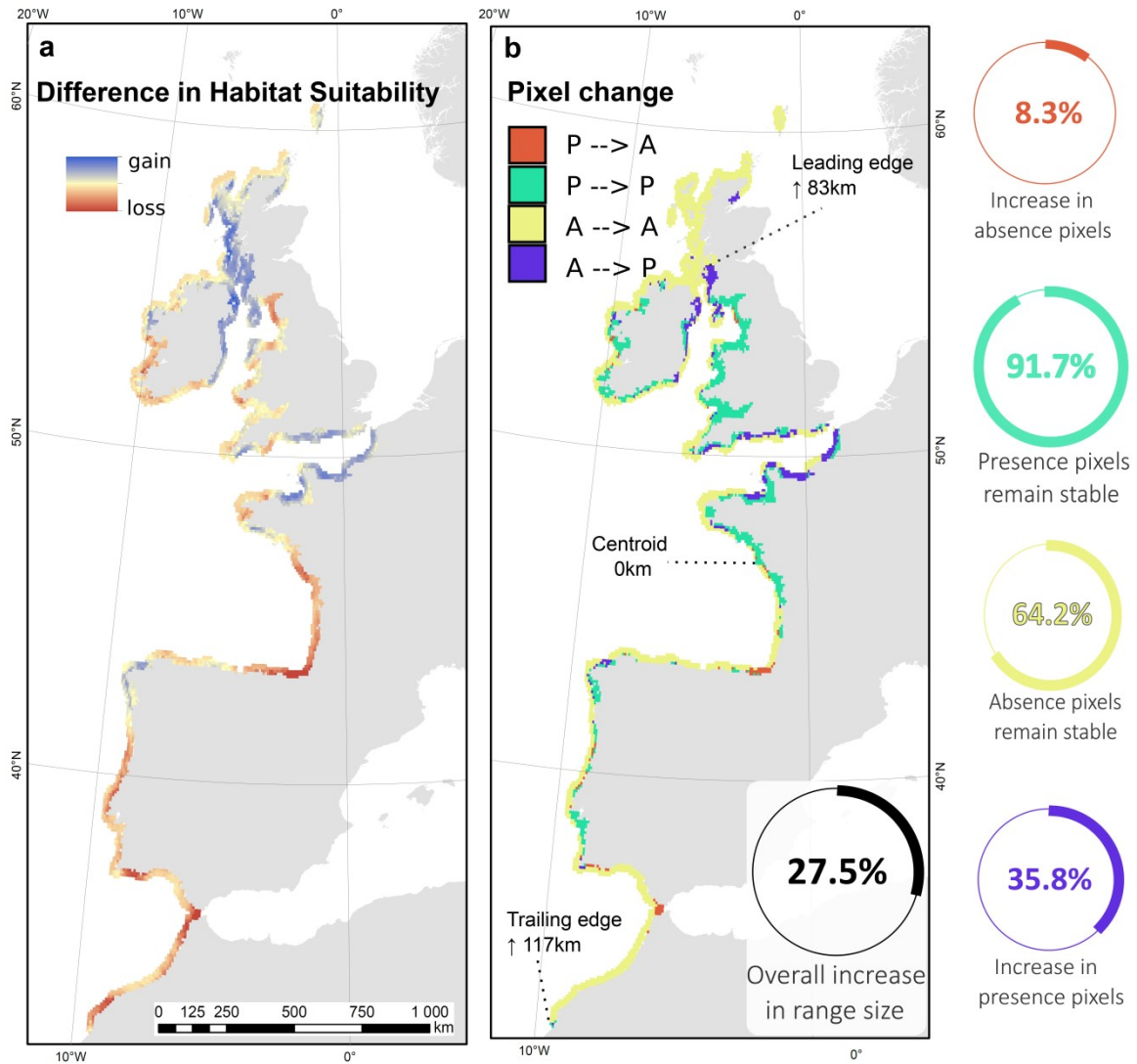
363 **3 | RESULTS**

364 **3.1 | Model performance and variable importance**

365 Ensemble model predictions of present distribution performed well (AUC = 0.91 ± 0.03 ; TSS =
366 0.67 ± 0.05 - Table S2 and Figure S10) in characterising the large-scale, yet fragmented,
367 latitudinal range of *S. alveolata* (specificity score 0.78 ± 0.06 ; Figure 3a). Predicted areas of
368 absence (e.g. southern French Atlantic coast) also matched well with current observed
369 absence data (Figures 2a and 3a, Figure S1). Fetch was the most important variable
370 (explaining 35% of variance), suggesting that coastal exposure to wind-wave action, a local to
371 regional scale feature, is a primary determinant of habitat suitability (Table S3 and Figure S7).
372 Dynamic temperature variables and ocean variables had less influence on model predictions
373 but were still critical to characterise broad-scale geographic range. In fact, sea surface and air
374 temperature were the second and fourth most important variables, respectively, while salinity

375 was the third most important variable (Table S3). See Figure S11 for variable response
376 curves.

377



378

379 **FIGURE 3 Predicted difference in habitat suitability and presence-absence patterns**
380 **between current and future (RCP 4.5 2050) climatic conditions. a**, Difference in habitat
381 suitability between present and future, with blue colours indicating a future increase in habitat
382 suitability, and red colours indicating a future loss in habitat suitability (yellow colours
383 represent an absence of change). **b**, Change in presence/absence predictions between the
384 present and future. Orange pixels (P -> A) = shift from current presence to future absence;
385 green pixels (P -> P) = stable presence pixels; yellow pixels (A -> A) = stable absence pixels;
386 violet pixels (A -> P) = shift from current absence to future presence. Predictions were

387 binarised using a max TSS threshold of 0.53. Leading edge = 95% quantile of the latitudinal
388 range, Trailing edge = 5% quantile of the latitudinal range, centroid = range centre/optimum
389 median.

390

391 **3.2 | Broad-scale range changes**

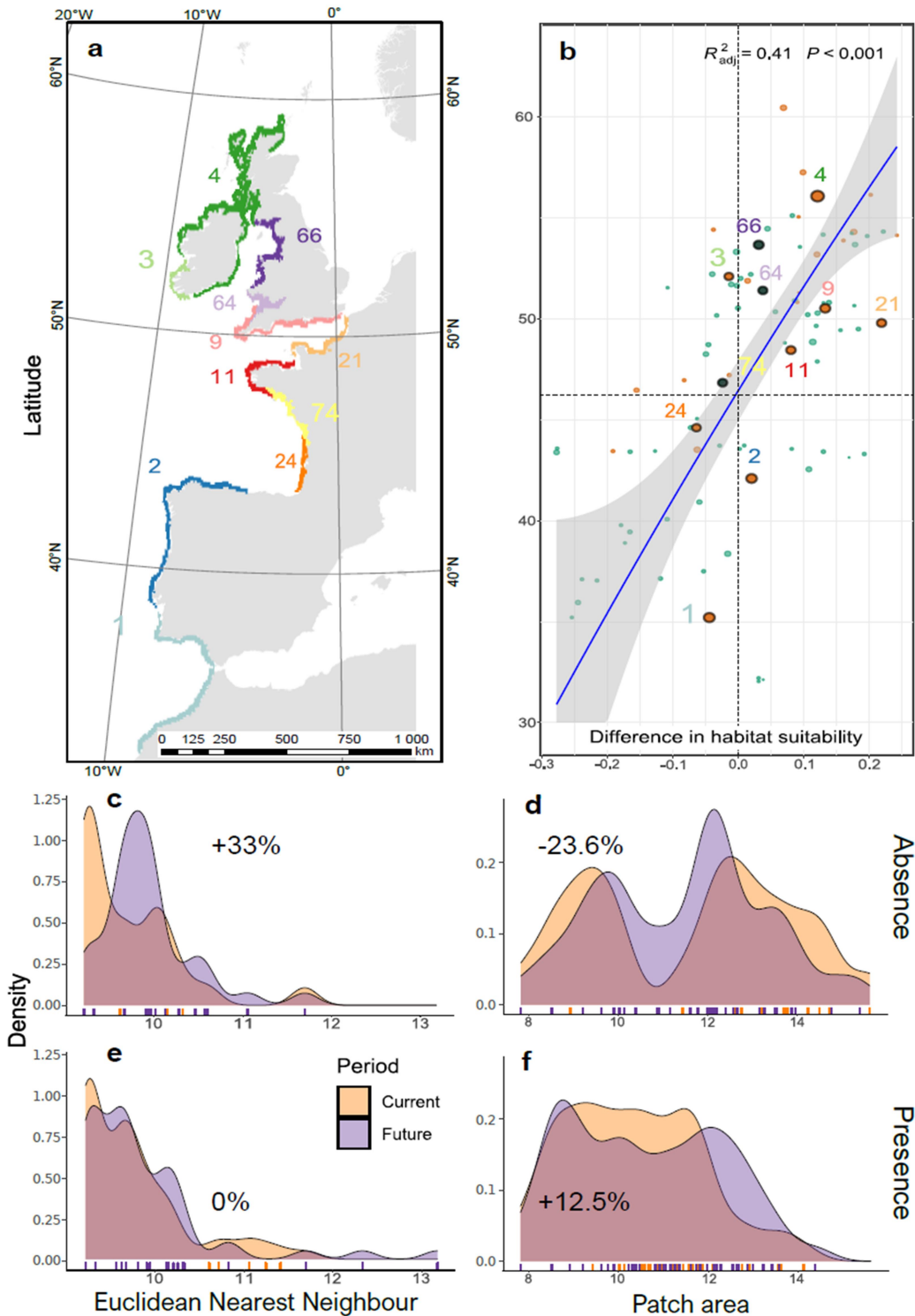
392 The ensemble model predicts a 27.5% increase in range size (Figure 3b), with future gains
393 predicted to mostly occur around the Irish Sea, on both sides of the English Channel and
394 along the coast of Galicia (Spain) (Figure 3a). Overall, we found large spatial heterogeneity in
395 the proportion of pixels predicted to become suitable (35.8%), unsuitable (8.3%) and stable
396 (91.7% of absence pixels and 64.2% of presence pixels) in the future (Figure 3b). This
397 heterogeneity leads to an overall contraction of the latitudinal range owing to a greater
398 retraction of the trailing edge relative to the extension of the leading edge (117 km vs. 83 km
399 respectively; Table S4, Figure 3b). Although other local changes are visible, they are not
400 captured by broad-scale range metrics.

401

402 **3.3 | Within-range changes**

403 The application of landscape metrics enabled us to identify 90 patches (both presences and
404 absences) in the current time period, and 92 patches in the future. While mean habitat
405 suitability per patch increased with latitude ($P < 0.001$; $R^2 = 0.41$), 59% of the variability in
406 patch suitability remained unexplained, highlighting departures from expectations (i.e. a
407 global poleward shift).

408



409

410 **FIGURE 4 Overview of presence-absence patches and changes between time periods for**
 411 **selected patch and landscape metrics. a**, Map of 2000-2019 presence/absence patches.
 412 Numbered regions map to their equivalent 'bubbles' in (b). **b**, Change in average patch habitat
 413 suitability between current (2000-2019) and future (RCP 4.5 2040-2049) as a function of
 414 latitude. Current presence patches are displayed in green whereas current absence patches are
 415 in orange. Bubble size indicates patch area. The horizontal dashed line points to the latitude at

416 which the predicted difference in habitat suitability switches from negative to positive.
417 Latitude was treated as the independent variable but the axes were flipped for presentation
418 purposes. Density plots highlighting changes in patch level Euclidean nearest neighbour
419 (ENN) distance for both absence (c) and presence patches (e), whilst (d) and (f) show the
420 change in patch area for absences and presences respectively. For each density plot, the
421 proportional change between future and current median values, relative to the current period,
422 are highlighted.

423

424 Despite an overall stability in the total number of patches between current and future
425 conditions, presence patches are predicted to decrease from 65 to 56 (-14%), while absence
426 patches are predicted to increase from 25 to 36 (+31%) (Figures S12 and S13). This does not
427 however mean that absences are more prevalent in the future, owing to a global increase in the
428 size of presence patches (+12.5%) combined with a decrease in the size of absence patches (-
429 23.6%) (Figures 4d and 4f). The average distance (Euclidean nearest neighbour; Figures 4c
430 and 4e) between patches is predicted to increase in the future for absences (+33%) but to
431 remain stable for presences. The geographic distribution of presence and absence patches is
432 also predicted to change. For instance, presence patches are predicted to coalesce poleward,
433 with the formation of a large presence patch along the west coast of Britain and Ireland, while
434 most equatorward patches are predicted to fragment (Figures 3b and 4e).

435 Future predictions show that patches can behave in one of four ways. Either presence and
436 absence patches can expand, or patches of presence can appear in areas of absence and vice-
437 versa. An example of each specific case is presented in Figure 5, with associated local-scale
438 landscape metrics. Note that these metrics can be obtained within any section of the range.
439 For instance, when considering the southwest coast of England, we predict that five presence
440 patches will merge into one larger presence patch in the future owing to multiple absence
441 pixels predicted to become suitable (Figure 5b). Focusing on this region, this change leads to
442 a 400% increase in the Largest Patch Index (LPI), the largest presence patch dominating 20%

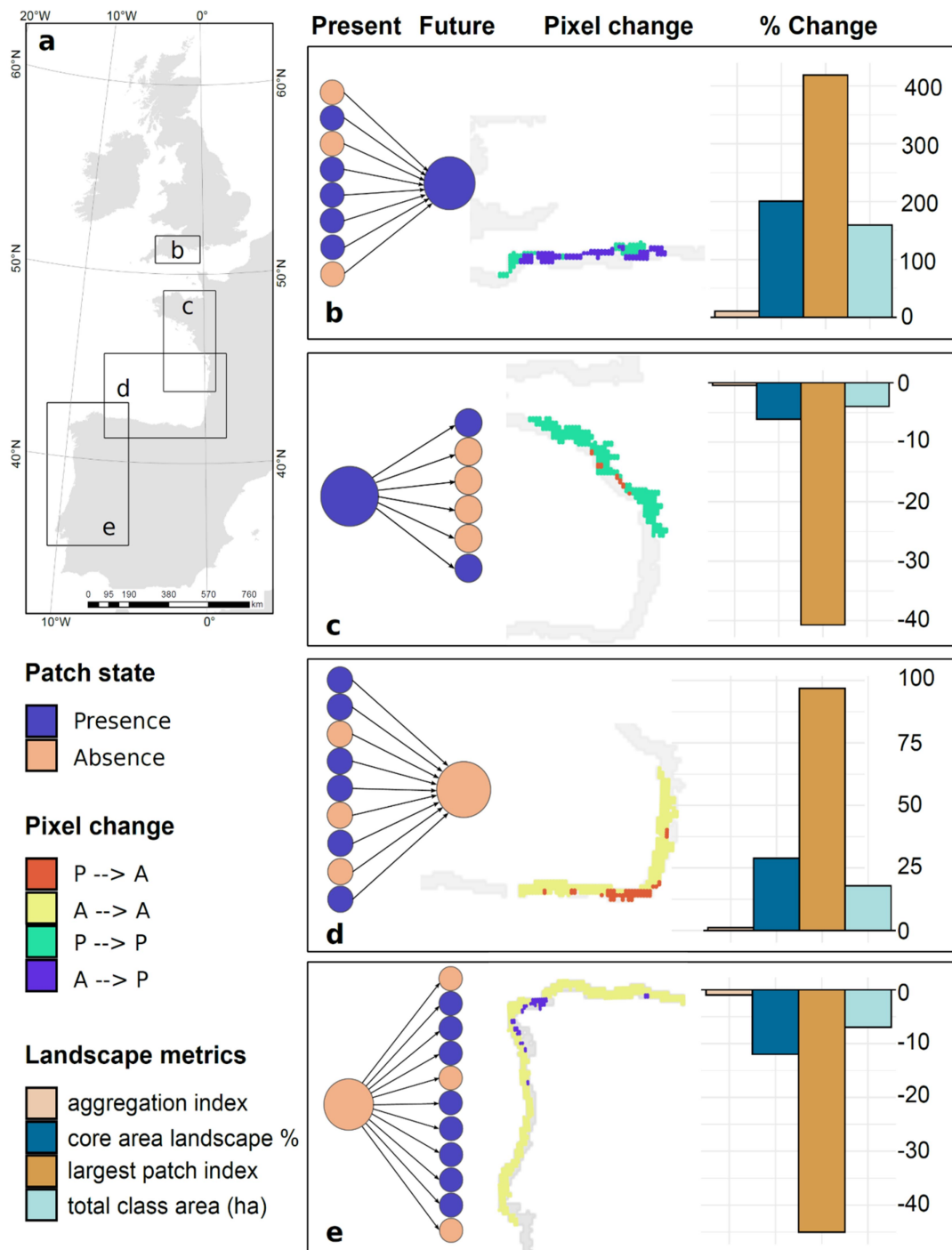
443 of this regional landscape under current conditions, and 100% under future conditions. In the
444 current range centre (north Bay of Biscay), we predict a localised extirpation in the centre of a
445 large presence patch (Figure 5c), increasing edge pixels between presence and absence
446 patches and thus decreasing the percent of core area (-6%). In northern Spain and the southern
447 Bay of Biscay, we predict the disappearance of small presence patches within a large absence
448 area (Figure 5d), increasing the total area of absences by nearly 18% within this region (total
449 class area metric). Finally, along the northwest Iberian Peninsula, numerous small areas of
450 suitable habitat are predicted to appear in a currently large absence patch (Figure 5e), leading
451 to a 1% decrease in aggregation index (from 86% under current conditions to 85% in the
452 future).

453

454 **4 | DISCUSSION**

455 In this study, we aimed to illustrate how and to what extent broad-scale metrics, that mostly
456 describe external range changes, can overlook the more nuanced internal range changes that
457 can take place under climate change. For this purpose, we focused on changes predicted under
458 current and future (2000-2019 vs. 2040-2049) environmental conditions for a species with a
459 naturally discontinuous distribution: *Sabellaria alveolata*. We then investigated how broad-
460 scale range metrics can be complemented by landscape metrics to better characterise the
461 effect climate change can have on species geographic ranges. Overall, we found that broad-
462 scale range metrics alone would have led to the conclusion that the study species is a climate
463 change winner. Within-range changes provided additional insights by revealing that the range
464 will become increasingly fragmented in its equatorward half in the future, with potential
465 implications for local declines and extirpations. As *S. alveolata* underpins myriad ecosystem
466 functions (Dubois et al., 2002; Jones et al., 2018) changes in its distribution (i.e. presence-

467 absence, hence occupancy of suitable habitats) and abundance are likely to have adverse
 468 cascading effects on ecosystem services (Wetthey et al., 2011).



469

470 **FIGURE 5 Examples of internal range change.** The four types of patch transitions, with
 471 barplots of associated landscape metrics. **a**, Location of all four examples. **b**, Expansion of
 472 presence patches **c**, Absence patches appearing in a larger presence patch. **d**, Expansion of
 473 absence patches. **e**, Presence patches appearing in a large absence patch. The barplots
 474 represent relative changes in different landscape metrics relative to baseline metrics calculated

475 under current environmental conditions: negative values indicate a decrease of the metric in
476 the future and positive values indicate the opposite. In all four examples, the coloured pixels
477 define the landscape on which the metrics are computed. The largest patch index is the
478 percentage of the landscape covered by the largest patch. The aggregation index describes the
479 extent to which patches of the same class are aggregated. The total class area is the sum of the
480 area of all patches of the same class. Finally, the core area landscape is the average of the
481 percentage of core area (i.e. patch area without edge pixels) in relation to total patch area.

482

483 Despite the recognised ecological and economic value of ecosystem engineers in terms of
484 biodiversity and ecosystem functioning (Ellison et al., 2005; Lemasson et al., 2017), to our
485 knowledge, only a handful of studies have simultaneously considered terrestrial and marine
486 environmental conditions to which coastal ecosystems are exposed (e.g. Lima et al., 2013;
487 Boo et al., 2019); so far only one study has focused on an ecosystem engineer (Faroni-Perez,
488 2017). Our results confirm that both air and seawater temperatures are ultimate drivers of
489 changes in sabellarid distribution (Faroni-Perez, 2017; Firth et al., 2015; Firth et al., 2021a),
490 thus confirming its status as an indicator of climate change in Britain and Ireland
491 (Mieszkowska et al., 2006). However, patterns of change are predicted to differ between
492 biogeographic regions owing to the effect of other local factors (Firth et al., 2021a). For
493 instance, our study suggests that the effect of temperature can be overridden by local and
494 regional factors determined by coastline orientation, especially due to fetch.

495 While the overall increase of habitat suitability predicted by SDM would categorise *S.*
496 *alveolata* as a climate change ‘winner’ (Somero, 2010), a closer look at SDM predictions
497 highlights a more nuanced situation owing to a complex interplay of various factors. First, *S.*
498 *alveolata* is predicted to reach the very north of Britain and Ireland by 2050, but in the longer-
499 term future (e.g. the 2090s), its poleward expansion will be limited by the lack of continuous
500 or connected landmass, as is the case for a number of other coastal species in northwest
501 Europe (Philippart et al., 2011). Some longer-term colonisation of the outer islands of the

502 British Isles (Hebrides, Orkney, Shetland) might be possible, but may be dispersal-limited.
503 This suggests that proximate factors such as habitat availability (supply of sand for tube
504 building adjacent to hard substrata for adhesion) and dispersal ability may override the
505 ultimate drive of climate change (Harley et al., 2006). Second, the predicted shrink of the
506 latitudinal range (Figure 3b) indicates that the distribution will be mostly clustered in
507 poleward regions but increasingly fragmented in equatorward regions (Figure 4), a process
508 that could disrupt connectivity networks between isolated populations. This is particularly
509 concerning in the equatorward part of *S. alveolata*'s range given that it is currently located
510 within the Canary Eastern Boundary Upwelling System, where a rapid warming at its trailing
511 edge is occurring ($0.60^{\circ}\text{C decade}^{-1}$ off Mauritania), leading to speculation that an upwelling
512 shutdown or geographic shift has already begun (Seabra et al., 2019). This pattern matches
513 well with previous findings showing that leading (poleward) and trailing (equatorward) edges
514 respond differently to climate change (Poloczanska et al., 2013). At the leading edge, larger
515 occurrence patches could strengthen regional connectivity, which could favour inter-seeding
516 between distant populations and enhance species regional resilience to local perturbations or
517 extreme climatic events. In contrast, at the trailing edge, increased distance between presence
518 patches could lead to a loss of genetic diversity in threatened former core areas of the range
519 (Nicastro et al., 2013). Thus, while some presence patches located at the trailing edge are
520 predicted to increase in habitat suitability (e.g. the patch located close to Morocco is predicted
521 to increase from 0.53 to 0.57), their increasing isolation could actually lead to an increased
522 extirpation risk. If this happens, the trailing edge would shift to southern Spain (Gulf of
523 Cadiz), leading to a further range contraction of 500 km. Third, while trailing and leading
524 edges are clearly identified by SDM predictions, our model further predicts a strong decrease
525 in habitat suitability in the central part of the range along the French Atlantic coast (Figure
526 3c), a critical region for this species where it forms extensive reefs (surface cover (100s ha)

527 and height (>1m)) (Curd et al., 2020). A decrease in habitat suitability in this region could
528 lead to a break in connectivity between the equatorward and poleward parts of the range,
529 should the gap between the two regions exceed the dispersal abilities of the species (Wort et
530 al., 2019).

531 The three preceding points suggest that *S. alveolata* may not, at a global scale, be a climate
532 change winner. Up until now, such detailed changes required expert knowledge and a deep
533 understanding of the ecology of the focal species, which are very difficult to attain
534 particularly in multi-species studies. We propose to use additional landscape metrics,
535 transposable from one species to another, to adequately and generically describe the complex
536 changes taking place within species ranges. While not replacing the critical value of expert-
537 based interpretations, this approach could help pinpoint more complex changes than the ones
538 reported with broad-scale range metrics. Overall, our results indicate that landscape metrics,
539 and particularly the Euclidean nearest neighbour distance between patches of the same class,
540 are valuable to identify vulnerable and isolated patches, and can help inform regional
541 management strategies (e.g. promoting ecological connectivity among populations). For
542 instance, the identification of isolated patches could be used to locate further work on larval
543 dispersal and recruitment, along with genetic diversity studies to help understand how
544 separate patches of presences are interconnected and therefore whether they are part of a
545 metapopulation functioning. Such studies are of particular interest given the role of isolated
546 populations in evolutionary processes (see Supplementary Text).

547 More generally, several landscape metrics could be used to describe the extent to which
548 various patch properties (e.g. area, aggregation patterns) are predicted to change in the future.
549 Similarly to global change metrics classically reported in SDMs studies, we encourage future
550 studies to report such internal range metrics to better predict climate change effects on species
551 ranges. Interestingly, these metrics can be calculated at different user-defined resolutions,

552 giving the possibility to study changes taking place at different spatial scales (e.g. regional,
553 global, Chase et al. 2018). The issue of scale is at the core of landscape ecology (Turner et al.
554 2005) and previous studies have reviewed its effects on landscape metrics (e.g. Newman et al.
555 2019). Applying landscape metrics to SDM outputs adds another layer of complexity, since
556 the accuracy of SDM predictions also varies depending on the spatial resolution and the scale
557 considered (e.g. Chauvier et al. 2022). Here, we defined a patch as a minimum of one isolated
558 pixel because of the broad-scale nature of the study. For finer-scale studies, a given number of
559 pixels per patch could be set as a threshold. The latter could be based on ecological
560 knowledge (e.g. dispersal distance), or by setting arbitrary thresholds and subsequently
561 conducting a sensitivity analysis. Beyond landscape metrics, the fact that patches and
562 associated pixels are characterised by unique identifiers further makes it possible to study in
563 more detail (e.g. regional or species-centred studies) how patches of presences and absences
564 are predicted to fragment or coalesce in the future. For instance, despite the stable number of
565 patches predicted in the future, multiple colonisation and extinction events are predicted
566 throughout the range, leading to current patches (of presences or absences) either splitting into
567 several patches or merging with existing patches (Figure 5, Figures S12 and S13, Table S5).
568 The predicted merging of presence patches in southwest England suggests that greater
569 dispersion among existing presence patches in this area could either foster a range expansion,
570 or resilience increase. In the current range centre (north Bay of Biscay), we predict a localised
571 extirpation in the centre of a large presence patch, leading to a future gap between two
572 presence patches. Similarly, between trailing edge populations (northern Spain) and
573 populations from the Bay of Biscay, we predict local extirpations of a potential key stepping-
574 stone population within a large absence area, with potential implications for connectivity.
575 Finally, the predicted appearance of several small patches of suitable habitat within a
576 currently large absence patch along the northwest Iberian Peninsula reinforces the importance

577 of conservation efforts covering small habitat areas, as integrating key fragments in coastal
578 management could benefit long-term species persistence. Beyond population connectivity, the
579 predicted changes in spatial configuration may alter ecosystem functioning and dynamics.
580 Spatial configurations are intrinsically linked with regime stability or shifts (Kefi et al., 2014).
581 Landscape metrics can provide information on internal range changes which can act as early
582 warning signals of impending regime shifts (Nijp et al., 2019). Relatively simple statistical
583 landscape metrics are therefore critical for conservation, and could perhaps even fuel other
584 types of analysis aiming to understand spatial early warning signals as ecosystems approach a
585 tipping point (Génin et al., 2018).

586 The extirpation of ecosystem engineers and the related cascading ecosystem effects are
587 considered principal drivers of regime shifts in both marine and terrestrial realms (Estes et al.,
588 2018; Wright, 2009). There are, however, also consequences when the range of an ecosystem
589 engineer shifts due to climate change, enabling colonisation of individuals and persistence of
590 populations into new areas. The potential gain of an extensive area of suitable habitat, in
591 Britain and Ireland, could alter community structure and ecosystem processes, with ensuing
592 positive and negative impacts (Bulleri et al., 2018; Wallingford et al., 2020). It is also possible
593 that species inhabiting *S. alveolata* reefs will exhibit range extensions by using the new areas
594 of reef occurrence as “stepping stones”, with climate change facilitating the dispersion of the
595 associated biota into new territories (Dubois et al., 2002; Faroni-Perez 2017), aided by
596 proliferating sea defences as a societal adaptational response to rising and stormier seas driven
597 by climate change (Bugnot et al., 2021; Firth et al., 2015). As a biogenic habitat forming
598 species, it could also promote the diversity and resilience of benthic fauna by providing
599 improved environmental conditions in the face of climate change through facilitation or
600 habitat cascades (Bulleri et al., 2018; Gribben et al., 2019). The duality of effects upon
601 recipient communities underscores the importance of considering the ecological impacts of

602 species exhibiting range-shifts, in terms of both the benefits and potential costs to associated
603 biodiversity and ecosystem functioning and service provision (Wallingford et al., 2020).
604 Despite fundamental differences between introduced non-native and naturally range-shifting
605 species, they can impact communities via analogous mechanisms (Wallingford et al., 2020).
606 Landscape metrics could therefore also be useful for invasion risk assessments at a spatial
607 scale relevant to regional and local-scale management decisions, e.g. Marine Protected Areas.

608 Several studies have used landscape metrics as covariates in SDMs to improve model
609 predictions (Hasui et al., 2017; Ortner & Wallentin 2020). The novelty in our approach lies in
610 the application of landscape metrics to binary predictions obtained from SDMs (or any spatial
611 model e.g. joint-SDMs or mechanistic models) in order to identify patches of absences and
612 presences. This framework makes it possible to study the internal range structure of species
613 and better characterise the evolution of species ranges in response to e.g. climate change,
614 provided that predictions are robust (i.e. our approach does not circumvent the flaws inherent
615 to spatial models and does not improve their accuracy). For instance, selected landscape
616 metrics can either reinforce or hinder the conclusions drawn from global change metrics.

617 Here, we have shown a global increase in the range area (+27%) but further found that this
618 global increase was mostly due to one presence patch largely increasing in the northern part of
619 the range (coalescing with other presence patches) while most other presence patches were
620 collapsing. While providing some avenues regarding how changes in landscape metrics could
621 be interpreted when applied to SDMs outputs, the choice of landscape metrics and their
622 interpretation will ultimately depend on the study system and question. Here we focused on
623 the effect of climate change; however SDMs have been used for many other purposes (Bellard
624 et al. 2012) where the use of landscape metrics would still be valuable. For instance, patch
625 size and nearest neighbour metrics can be used jointly to identify patches that will become
626 increasingly isolated in the future and for which conservation actions may be needed.

627

628 5 | CONCLUSIONS

629 As Earth's climate rapidly changes, individuals of a species must move, acclimate, adapt, or
630 die. Range shifts are therefore key to species persistence (Muir et al., 2020). Beyond range
631 size and boundaries, internal range structure metrics are needed to adequately describe
632 species' ranges and more accurately quantify how they will be affected in the future (Csergő
633 et al., 2020), particularly for species with discontinuous distributions. Analysing which
634 landscape-level processes scale up to structure biogeographic ranges of species has however
635 remained largely unexplored. Recent work however provides evidence that population and
636 species level responses to habitat change at the landscape scale are modulated by factors and
637 processes occurring at macroecological scales, such as historical disturbance rates, distance to
638 geographic range edges, and climatic suitability (Banks-Leite et al., 2022). Our results suggest
639 that these landscape-scale processes may be key to understanding and predicting internal
640 range reconfiguration in changing environments. Specifically, we showed that broad-scale
641 SDM combining terrestrial and marine predictors, coupled with a selection of global and
642 regional landscape metrics, can be used to more accurately describe the changes a widely
643 distributed intertidal species will face. Fragmentation of occupied area or suitable habitat has
644 already been identified as a better predictor of extinction risk than range size (Crooks et al.,
645 2017), and we propose that metrics characterising different aspects of species range structure,
646 such as the distance between patches of suitable habitat, may be useful to meet conservation
647 targets.

648 Conservation efforts should be refocused to search for critical internal range structure
649 thresholds, especially those acting as proximate factors. Environmental management often
650 focuses on single sites and populations, which crucially do not consider the wider context.

651 Landscape metrics applied to SDM outputs are a robust, non-data-intensive method that can
652 aid environmental managers with broad-scale spatial planning under climate change.

653

654 **AUTHOR CONTRIBUTIONS**

655 A.C., L.B.F. and S.F.D. conceived this research. M.C., M.V., A.B. and M.P.M. analysed
656 species distribution data and developed the use of landscape metrics in combination with
657 SDM outputs to better characterize changes in species internal range structure. L.M.B, M.T.B
658 and J.A.M.G. provided the oceanographic data for wave, fetch and tide respectively. A.C.,
659 L.E.B., C.C., A.J.D., S.F.D., L.B.F., S.J.H., F.P.L., C.M., N.M. and R.S. contributed towards
660 the species distribution data. A.C. wrote the first draft. A.C., M.C., L.B.F., S.F.D., A.B., M.V.
661 and M.M. contributed equally to discussion of ideas and analyses. M.C., A.J.D., L.B.F. and
662 S.J.H. provided substantial inputs on drafts and revisions of the paper. All authors commented
663 on the manuscript.

664

665 **ACKNOWLEDGEMENTS**

666 We thank the many field assistants and citizen scientists who have gathered data on
667 *Sabellaria alveolata* along Europe's coastline over many years. AC was funded by a PhD
668 grant from Ifremer. This study was financially supported by the Total Foundation [Grant No.
669 1512 215 588/F, 2015]. The wave modelling was supported by the European Union's Seventh
670 Programme for Research, Technological Development, and Demonstration under grant
671 agreement FP7-ENV-2013-Two-Stage-603396-RISES-AM- and the ARCHER UK National
672 Supercomputing Service <http://www.archer.ac.uk>.

673

674 **CONFLICT OF INTEREST**

675 The authors declare that they have no competing interests.

676

677 DATA AVAILABILITY STATEMENT

678 The *S. alveolata* records dataset is archived as a .csv file in the SEANOE data repository
679 (<https://doi.org/10.17882/72164>). All sources of environmental predictors used for modelling
680 are freely available and referenced in Table S1. The code that supports the findings of this
681 study is available from https://github.com/Mathieu-Chevalier/SDM_landscape_metrics

682 REFERENCES

683 Alhajeri, B. H., & Fourcade, Y. (2019). High correlation between species-level environmental
684 data estimates extracted from IUCN expert range maps and from GBIF occurrence data.
685 *Journal of Biogeography*, 46(7), 1329–1341.

686 Allouche, O., Tsoar, A., & Kadmon, R. (2006). Assessing the accuracy of species distribution
687 models: Prevalence, kappa and the true skill statistic (TSS): Assessing the accuracy of
688 distribution models. *Journal of Applied Ecology*, 43(6), 1223–1232.

689 <https://doi.org/10.1111/j.1365-2664.2006.01214.x>

690 Araújo, M. B., Anderson, R. P., Márcia Barbosa, A., Beale, C. M., Dormann, C. F., Early, R.,
691 Garcia, R. A., Guisan, A., Maiorano, L., Naimi, B., O'Hara, R. B., Zimmermann, N. E.,
692 & Rahbek, C. (2019). Standards for distribution models in biodiversity assessments.

693 *Science Advances*, 5(1), eaat4858. <https://doi.org/10.1126/sciadv.aat4858>

694 Assis, J., Tyberghein, L., Bosch, S., Verbruggen, H., Serrão, E. A., & De Clerck, O. (2018).

695 Bio-ORACLE v2.0: Extending marine data layers for bioclimatic modelling. *Global*

696 *Ecology and Biogeography*, 27(3), 277–284. <https://doi.org/10.1111/geb.12693>

697 Banks-Leite, C., Betts, M. G., Ewers, R. M., Orme, C. D. L., & Pigot, A. L. (2022). The
698 macroecology of landscape ecology. *Trends in Ecology & Evolution*,
699 S0169534722000052. <https://doi.org/10.1016/j.tree.2022.01.005>

700 Barbet-Massin, M., Jiguet, F., Albert, C. H., & Thuiller, W. (2012). Selecting pseudo-
701 absences for species distribution models: How, where and how many?: How to use
702 pseudo-absences in niche modelling? *Methods in Ecology and Evolution*, 3(2), 327–
703 338. <https://doi.org/10.1111/j.2041-210X.2011.00172.x>

704 Barbier, E. B., Hacker, S. D., Kennedy, C., Koch, E. W., Stier, A. C., & Silliman, B. R.
705 (2011). The value of estuarine and coastal ecosystem services. *Ecological Monographs*,
706 81(2), 169–193.

707 Beaumont, L. J., Graham, E., Duursma, D. E., Wilson, P. D., Cabrelli, A., Baumgartner, J. B.,
708 Hallgren, W., Esperón-Rodríguez, M., Nipperess, D. A., & Warren, D. L. (2016).
709 Which species distribution models are more (or less) likely to project broad-scale,
710 climate-induced shifts in species ranges? *Ecological Modelling*, 342, 135–146.

711 Boo, G. H., Qiu, Y., Kim, J. Y., Ang, P. O., Bosch, S., De Clerck, O., He, P., Higa, A.,
712 Huang, B., Kogame, K., Liu, S., Nguyen, T., Suda, S., Terada, R., Miller, K. A., & Boo,
713 S. M. (2019). Contrasting patterns of genetic structure and phylogeography in the
714 marine agarophytes *Gelidiophycus divaricatus* and *G. Freshwateri* (Gelidiales,
715 Rhodophyta) from East Asia¹. *Journal of Phycology*, jpy.12910.
716 <https://doi.org/10.1111/jpy.12910>

717 Breiman, L. (2001). Random forests. *Machine Learning*, 45(1), 5–32.

718 Bricheno, L. M., & Wolf, J. (2018). Future Wave Conditions of Europe, in Response to High-
719 End Climate Change Scenarios. *Journal of Geophysical Research: Oceans*, 123(12),
720 8762–8791. <https://doi.org/10.1029/2018JC013866>

721 Bučas, M., Bergström, U., Downie, A.-L., Sundblad, G., Gullström, M., von Numers, M.,
722 Šiaulys, A., & Lindegarth, M. (2013). Empirical modelling of benthic species
723 distribution, abundance, and diversity in the Baltic Sea: Evaluating the scope for
724 predictive mapping using different modelling approaches. *ICES Journal of Marine*
725 *Science*, 70(6), 1233–1243. <https://doi.org/10.1093/icesjms/fst036>

726 Bugnot, A. B., Mayer-Pinto, M., Airoidi, L., Heery, E. C., Johnston, E. L., Critchley, L. P.,
727 Strain, E. M. A., Morris, R. L., Loke, L. H. L., Bishop, M. J., Sheehan, E. V., Coleman,
728 R. A., & Dafforn, K. A. (2021). Current and projected global extent of marine built
729 structures. *Nature Sustainability*, 4(1), 33–41. [https://doi.org/10.1038/s41893-020-](https://doi.org/10.1038/s41893-020-00595-1)
730 [00595-1](https://doi.org/10.1038/s41893-020-00595-1)

731 Bulleri, F., Eriksson, B. K., Queirós, A., Airoidi, L., Arenas, F., Arvanitidis, C., Bouma, T. J.,
732 Crowe, T. P., Davoult, D., Guizien, K., Iveša, L., Jenkins, S. R., Michalet, R., Olabarria,
733 C., Procaccini, G., Serrão, E. A., Wahl, M., & Benedetti-Cecchi, L. (2018). Harnessing
734 positive species interactions as a tool against climate-driven loss of coastal biodiversity.
735 *PLOS Biology*, 16(9), e2006852. <https://doi.org/10.1371/journal.pbio.2006852>

736 Burrows, M. T., Hawkins, S. J., Moore, J. J., Adams, L., Sugden, H., Firth, L., &
737 Mieszkowska, N. (2020). Global-scale species distributions predict temperature-related
738 changes in species composition of rocky shore communities in Britain. *Global Change*
739 *Biology*, gcb.14968. <https://doi.org/10.1111/gcb.14968>

740 Burrows, M. (2020). *Wave fetch GIS layers for Europe at 100m scale* (p. 904169794 Bytes)
741 [Data set]. figshare. <https://doi.org/10.6084/M9.FIGSHARE.8668127>

742 Calabrese, J. M., Certain, G., Kraan, C., & Dormann, C. F. (2014). Stacking species
743 distribution models and adjusting bias by linking them to macroecological models:
744 Stacking species distribution models. *Global Ecology and Biogeography*, 23(1), 99–
745 112. <https://doi.org/10.1111/geb.12102>

746 Chase, J. M., McGill, B. J., McGlinn, D. J., May, F., Blowes, S. A., Xiao, X., Knight, T. M.,
747 Purschke, O., & Gotelli, N. J. (2018). Embracing scale-dependence to achieve a deeper
748 understanding of biodiversity and its change across communities. *Ecology Letters*,
749 21(11), 1737–1751. <https://doi.org/10.1111/ele.13151>

750 Chauvier, Y., Descombes, P., Guéguen, M., Boulangeat, L., Thuiller, W., & Zimmermann, N.
751 E. (2022). Resolution in species distribution models shapes spatial patterns of plant
752 multifaceted diversity. *Ecography*. <https://doi.org/10.1111/ecog.05973>

753 Cianfrani, C., Broennimann, O., Loy, A., & Guisan, A. (2018). More than range exposure:
754 Global otter vulnerability to climate change. *Biological Conservation*, 221, 103–113.
755 <https://doi.org/10.1016/j.biocon.2018.02.031>

756 Crooks, K. R., Burdett, C. L., Theobald, D. M., King, S. R., Di Marco, M., Rondinini, C., &
757 Boitani, L. (2017). Quantification of habitat fragmentation reveals extinction risk in
758 terrestrial mammals. *Proceedings of the National Academy of Sciences*, 114(29), 7635–
759 7640.

760 Csergő, A. M., Broennimann, O., Guisan, A., & Buckley, Y. M. (2020). Beyond range size:
761 Drivers of species' geographic range structure in European plants. *BioRxiv*,
762 2020.02.08.939819. <https://doi.org/10.1101/2020.02.08.939819>

763 Curd, A., Pernet, F., Corporeau, C., Delisle, L., Firth, L. B., Nunes, F. L. D., & Dubois, S. F.
764 (2019). Connecting organic to mineral: How the physiological state of an ecosystem-
765 engineer is linked to its habitat structure. *Ecological Indicators*, 98, 49–60.
766 <https://doi.org/10.1016/j.ecolind.2018.10.044>

767 Curd, A., Cordier, C., Firth, L. B., Bush, L., Gruet, Y., Le Mao, P., Blaze, J. A., Board, C.,
768 Bordeyne, F., Burrows, M. T., Cunningham, P. N., Davies, A. J., Desroy, N., Edwards,
769 H., Harris, D. R., Hawkins, S. J., Kerckhof, F., Lima, F. P., McGrath, D., ... Dubois, S.
770 (2020). *A broad-scale long-term dataset of Sabellaria alveolata distribution and*

771 *abundance curated through the REEHAB (REEf HABitat) Project* [Data set]. SEANOE.
772 <https://doi.org/10.17882/72164>

773 de la Hoz, C. F., Ramos, E., Puente, A., & Juanes, J. A. (2019). Temporal transferability of
774 marine distribution models: The role of algorithm selection. *Ecological Indicators*, *106*,
775 105499. <https://doi.org/10.1016/j.ecolind.2019.105499>

776 Dubois, S., Retière, C., & Olivier, F. (2002). Biodiversity associated with Sabellaria alveolata
777 (Polychaeta: Sabellariidae) reefs: effects of human disturbances. *Journal of the Marine*
778 *Biological Association of the UK*, *82*(5), 817–826.
779 <https://doi.org/10.1017/S0025315402006185>

780 Ellison, A. M., Bank, M. S., Clinton, B. D., Colburn, E. A., Elliott, K., Ford, C. R., Foster, D.
781 R., Kloeppe, B. D., Knoepp, J. D., & Lovett, G. M. (2005). Loss of foundation species:
782 Consequences for the structure and dynamics of forested ecosystems. *Frontiers in*
783 *Ecology and the Environment*, *3*(9), 479–486.

784 Elith*, J., H. Graham*, C., P. Anderson, R., Dudík, M., Ferrier, S., Guisan, A., J. Hijmans, R.,
785 Huettmann, F., R. Leathwick, J., & Lehmann, A. (2006). Novel methods improve
786 prediction of species' distributions from occurrence data. *Ecography*, *29*(2), 129–151.

787 Elith, J., Leathwick, J. R., & Hastie, T. (2008). A working guide to boosted regression trees.
788 *Journal of Animal Ecology*, *77*(4), 802–813.

789 Egbert, G. D., & Erofeeva, S. Y. (2002). Efficient Inverse Modeling of Barotropic Ocean
790 Tides. *Journal of Atmospheric and Oceanic Technology*, *19*(2), 183–204.
791 [https://doi.org/10.1175/1520-0426\(2002\)019<0183:EIMOBO>2.0.CO;2](https://doi.org/10.1175/1520-0426(2002)019<0183:EIMOBO>2.0.CO;2)

792 Egbert, G. D., Erofeeva, S. Y., & Ray, R. D. (2010). Assimilation of altimetry data for
793 nonlinear shallow-water tides: Quarter-diurnal tides of the Northwest European Shelf.
794 *Continental Shelf Research*, *30*(6), 668–679. <https://doi.org/10.1016/j.csr.2009.10.011>

795 Estes, L., Elsen, P. R., Treuer, T., Ahmed, L., Caylor, K., Chang, J., Choi, J. J., & Ellis, E. C.
796 (2018). The spatial and temporal domains of modern ecology. *Nature Ecology &*
797 *Evolution*, 2(5), 819–826. <https://doi.org/10.1038/s41559-018-0524-4>

798 Faroni-Perez, L. (2017). Climate and environmental changes driving idiosyncratic shifts in the
799 distribution of tropical and temperate worm reefs. *Journal of the Marine Biological*
800 *Association of the United Kingdom*, 97(05), 1023–1035.
801 <https://doi.org/10.1017/S002531541700087X>

802 Firth, L. B., Mieszkowska, N., Grant, L. M., Bush, L. E., Davies, A. J., Frost, M. T.,
803 Moschella, P. S., Burrows, M. T., Cunningham, P. N., Dye, S. R., & Hawkins, S. J.
804 (2015). Historical comparisons reveal multiple drivers of decadal change of an
805 ecosystem engineer at the range edge. *Ecology and Evolution*, 5(15), 3210–3222.
806 <https://doi.org/10.1002/ece3.1556>

807 Firth, L. B., Harris, D., Blaze, J. A., Marzloff, M. P., Boyé, A., Miller, P. I., Curd, A.,
808 Vasquez, M., Nunn, J. D., O'Connor, N. E., Power, A. M., Mieszkowska, N.,
809 O'Riordan, R. M., Burrows, M. T., Bricheno, L. M., Knights, A. M., Nunes, F. L. D.,
810 Bordeyne, F., Bush, L. E., ... Hawkins, S. J. (2021a). Specific niche requirements
811 underpin multidecadal range edge stability, but may introduce barriers for climate
812 change adaptation. *Diversity and Distributions*, 27(4), 668–683.
813 <https://doi.org/10.1111/ddi.13224>

814 Firth, L. B., Curd, A., Hawkins, Stephen. J., Knights, A. M., Blaze, J. A., Burrows, M. T.,
815 Dubois, S. F., Edwards, H., Foggo, A., Gribben, P. E., Grant, L., Harris, D.,
816 Mieszkowska, N., Nunes, F. L. D., Nunn, J. D., Power, A. M., O'Riordan, R. M.,
817 McGrath, D., Simkanin, C., & O'Connor, N. E. (2021b). On the diversity and
818 distribution of a data deficient habitat in a poorly mapped region: The case of *Sabellaria*

819 *alveolata* L. in Ireland. *Marine Environmental Research*, 105344.
820 <https://doi.org/10.1016/j.marenvres.2021.105344>

821 Frazier, A. E., & Kedron, P. (2017). Landscape Metrics: Past Progress and Future Directions.
822 *Current Landscape Ecology Reports*, 2(3), 63–72. [https://doi.org/10.1007/s40823-017-](https://doi.org/10.1007/s40823-017-0026-0)
823 [0026-0](https://doi.org/10.1007/s40823-017-0026-0)

824 Fredston-Hermann, A., Selden, R., Pinsky, M., Gaines, S. D., & Halpern, B. S. (2020). Cold
825 range edges of marine fishes track climate change better than warm edges. *Global*
826 *Change Biology*, 26(5), 2908–2922. <https://doi.org/10.1111/gcb.15035>

827 Gaston, K. J. (1996). Species-range-size distributions: Patterns, mechanisms and implications.
828 *Trends in Ecology & Evolution*, 11(5), 197–201.

829 Génin, A., Majumder, S., Sankaran, S., Danet, A., Guttal, V., Schneider, F. D., & Kéfi, S.
830 (2018). Monitoring ecosystem degradation using spatial data and the R package
831 *spatialwarnings*. *Methods in Ecology and Evolution*, 9(10), 2067–2075.
832 <https://doi.org/10.1111/2041-210X.13058>

833 Gribben, P. E., Angelini, C., Altieri, A. H., Bishop, M. J., Thomsen, M. S., & Bulleri, F.
834 (2019). Facilitation cascades in marine ecosystems: A synthesis and future directions. In
835 *Oceanography and Marine Biology*. Taylor & Francis.

836 Guisan, A., Thuiller, W., & Zimmermann, N. E. (2017). *Habitat suitability and distribution*
837 *models with applications in R*. Cambridge University Press.

838 Hanley, J. A., & McNeil, B. J. (1982). The meaning and use of the area under a receiver
839 operating characteristic (ROC) curve. *Radiology*, 143(1), 29-36.

840 Hao, T., Elith, J., Lahoz-Monfort, J. J., & Guillera-Aroita, G. (2020). Testing whether
841 ensemble modelling is advantageous for maximising predictive performance of species
842 distribution models. *Ecography*, 43(4), 549–558.

843 Harley, C. D. G., Randall Hughes, A., Hultgren, K. M., Miner, B. G., Sorte, C. J. B.,
844 Thornber, C. S., Rodriguez, L. F., Tomanek, L., & Williams, S. L. (2006). The impacts
845 of climate change in coastal marine systems: Climate change in coastal marine systems.
846 *Ecology Letters*, 9(2), 228–241. <https://doi.org/10.1111/j.1461-0248.2005.00871.x>

847 Hastie, T., & Tibshirani, R. (1986). Generalized Additive Models. *Statistical Science*, 1(3).
848 <https://doi.org/10.1214/ss/1177013604>

849 Heikkinen, R. K., Marmion, M., & Luoto, M. (2012). Does the interpolation accuracy of
850 species distribution models come at the expense of transferability? *Ecography*, 35(3),
851 276–288.

852 Helmuth, B., Mieszkowska, N., Moore, P., & Hawkins, S. J. (2006). Living on the Edge of
853 Two Changing Worlds: Forecasting the Responses of Rocky Intertidal Ecosystems to
854 Climate Change. *Annual Review of Ecology, Evolution, and Systematics*, 37(1), 373–
855 404. <https://doi.org/10.1146/annurev.ecolsys.37.091305.110149>

856 Hesselbarth, M. H., Sciaini, M., With, K. A., Wiegand, K., & Nowosad, J. (2019).
857 landscapemetrics: An open-source R tool to calculate landscape metrics. *Ecography*,
858 42(10), 1648–1657.

859 Hesselbarth, M. H. K., Nowosad, J., Signer, J., & Graham, L. J. (2021). Open-source Tools in
860 R for Landscape Ecology. *Current Landscape Ecology Reports*, 6(3), 97–111.
861 <https://doi.org/10.1007/s40823-021-00067-y>

862 Hijmans, R. J., Cameron, S. E., Parra, J. L., Jones, P. G., & Jarvis, A. (2005). Very high
863 resolution interpolated climate surfaces for global land areas. *International Journal of*
864 *Climatology*, 25(15), 1965–1978. <https://doi.org/10.1002/joc.1276>

865 Howell, P. E., Muths, E., Hossack, B. R., Sigafus, B. H., & Chandler, R. B. (2018). Increasing
866 connectivity between metapopulation ecology and landscape ecology. *Ecology*, 99(5),
867 1119–1128. <https://doi.org/10.1002/ecy.2189>

868 Hutchinson, G. E. (1978). *An introduction to population ecology* (Issue 504: 51 HUT).

869 Jones, A. G., Dubois, S. F., Desroy, N., & Fournier, J. (2018). Interplay between abiotic
870 factors and species assemblages mediated by the ecosystem engineer *Sabellaria*
871 *alveolata* (Annelida: Polychaeta). *Estuarine, Coastal and Shelf Science*, 200, 1–18.
872 <https://doi.org/10.1016/j.ecss.2017.10.001>

873 Kefi, S., Guttal, V., Brock, W. A., Carpenter, S. R., Ellison, A. M., Livina, V. N., Seekell, D.
874 A., Scheffer, M., van Nes, E. H., & Dakos, V. (2014). Early warning signals of
875 ecological transitions: Methods for spatial patterns. *PloS One*, 9(3), e92097.

876 Lausch, A., Blaschke, T., Haase, D., Herzog, F., Syrbe, R.-U., Tischendorf, L., & Walz, U.
877 (2015). Understanding and quantifying landscape structure – A review on relevant
878 process characteristics, data models and landscape metrics. *Use of Ecological*
879 *Indicators in Models*, 295, 31–41. <https://doi.org/10.1016/j.ecolmodel.2014.08.018>

880 Lawson, C. R., Hodgson, J. A., Wilson, R. J., & Richards, S. A. (2014). Prevalence,
881 thresholds and the performance of presence-absence models. *Methods in Ecology and*
882 *Evolution*, 5(1), 54–64. <https://doi.org/10.1111/2041-210X.12123>

883 Lemasson, A. J., Fletcher, S., Hall-Spencer, J. M. & Knights, A. M. (2017). Linking the biological
884 impacts of ocean acidification on oysters to changes in ecosystem services: a review. *Journal of*
885 *Experimental Marine Biology and Ecology*, 492, 49–62.
886 <https://doi.org/10.1016/j.jembe.2017.01.019>

887 Lenoir, J., Bertrand, R., Comte, L., Bourgeaud, L., Hattab, T., Murienne, J., & Grenouillet, G.
888 (2020). Species better track climate warming in the oceans than on land. *Nature*
889 *Ecology & Evolution*, 4, 1044–1059. <https://doi.org/10.1038/s41559-020-1198-2>

890 Lima, F. P., Ribeiro, P. A., Queiroz, N., Hawkins, S. J., & Santos, A. M. (2007). Do
891 distributional shifts of northern and southern species of algae match the warming
892 pattern? *Global Change Biology*, 13(12), 2592–2604.

893 Lourenço, C. R., Nicastró, K. R., McQuaid, C. D., Krug, L. A., & Zardi, G. I. (2020). Strong
894 upwelling conditions drive differences in species abundance and community
895 composition along the Atlantic coasts of Morocco and Western Sahara. *Marine*
896 *Biodiversity*, 50(2), 15. <https://doi.org/10.1007/s12526-019-01032-z>

897 McCullagh, P., & Nelder, J. A. (1998). *Generalized linear models* (2nd ed). Chapman &
898 Hall/CRC.

899 Meinshausen, M., Smith, S. J., Calvin, K., Daniel, J. S., Kainuma, M., Lamarque, J.-F.,
900 Matsumoto, K., Montzka, S., Raper, S., & Riahi, K. (2011). The RCP greenhouse gas
901 concentrations and their extensions from 1765 to 2300. *Climatic Change*, 109(1–2),
902 213.

903 Mestre, F., Risk, B. B., Mira, A., Beja, P., & Pita, R. (2017). A metapopulation approach to
904 predict species range shifts under different climate change and landscape connectivity
905 scenarios. *Ecological Modelling*, 359, 406–414.

906 Mieszkowska, N., Kendall, M., Hawkins, S., Leaper, R., Williamson, P., Hardman-
907 Mountford, N., & Southward, A. (2006). Changes in the range of some common rocky
908 shore species in Britain—A response to climate change? In *Marine Biodiversity* (pp.
909 241–251). Springer.

910 Mieszkowska, N., & Sugden, H. (2016). Climate-driven range shifts within benthic habitats
911 across a marine biogeographic transition zone. *Advances in Ecological Research*, 55,
912 325–369.

913 Muir, A. P., Dubois, S. F., Ross, R. E., Firth, L. B., Knights, A. M., Lima, F. P., Seabra, R.,
914 Corre, E., Le Corguillé, G., & Nunes, F. L. D. (2020). Seascape genomics reveals
915 population isolation in the reef-building honeycomb worm, *Sabellaria alveolata* (L.).
916 *BMC Evolutionary Biology*, 20(1), 100. <https://doi.org/10.1186/s12862-020-01658-9>

917 Naylor, L. A., & Viles, H. A. (2000). A temperate reef builder: An evaluation of the growth,
918 morphology and composition of *Sabellaria alveolata* (L.) colonies on carbonate
919 platforms in South Wales. *Geological Society, London, Special Publications*, 178(1), 9–
920 19.

921 Newman, E. A., Kennedy, M. C., Falk, D. A., & McKenzie, D. (2019). Scaling and
922 Complexity in Landscape Ecology. *Frontiers in Ecology and Evolution*, 7, 293.
923 <https://doi.org/10.3389/fevo.2019.00293>

924 Nicastro, K. R., Zardi, G. I., Teixeira, S., Neiva, J., Serrão, E. A., & Pearson, G. A. (2013).
925 Shift happens: Trailing edge contraction associated with recent warming trends
926 threatens a distinct genetic lineage in the marine macroalga *Fucus vesiculosus*. *BMC*
927 *Biology*, 11(1), 6. <https://doi.org/10.1186/1741-7007-11-6>

928 Nijp, J. J., Temme, A. J. A. M., Voorn, G. A. K., Kooistra, L., Hengeveld, G. M., Soons, M.
929 B., Teuling, A. J., & Wallinga, J. (2019). Spatial early warning signals for impending
930 regime shifts: A practical framework for application in real-world landscapes. *Global*
931 *Change Biology*, 25(6), 1905–1921. <https://doi.org/10.1111/gcb.14591>

932 Nunes, F. L. D., Rigal, F., Dubois, S. F., & Viard, F. (2021). Looking for diversity in all the
933 right places? Genetic diversity is highest in peripheral populations of the reef-building
934 polychaete *Sabellaria alveolata*. *Marine Biology*, 168(5), 63.
935 <https://doi.org/10.1007/s00227-021-03861-8>

936 Opdam, P., & Wascher, D. (2004). Climate change meets habitat fragmentation: Linking
937 landscape and biogeographical scale levels in research and conservation. *Biological*
938 *Conservation*, 117(3), 285–297.

939 Paquette, A., Hargreaves, A.L. (2021). Biotic interactions are more often important at species’
940 warm versus cool range edges. *Ecology Letters* 24, 2427–2438.
941 <https://doi.org/10.1111/ele.13864>

942 Parmesan, C., & Yohe, G. (2003). A globally coherent fingerprint of climate change impacts
943 across natural systems. *Nature*, 421(6918), 37–42.

944 Pecl, G. T., Araújo, M. B., Bell, J. D., Blanchard, J., Bonebrake, T. C., Chen, I.-C., Clark, T.
945 D., Colwell, R. K., Danielsen, F., Evengård, B., Falconi, L., Ferrier, S., Frusher, S.,
946 Garcia, R. A., Griffis, R. B., Hobday, A. J., Janion-Scheepers, C., Jarzyna, M. A.,
947 Jennings, S., ... Williams, S. E. (2017). Biodiversity redistribution under climate
948 change: Impacts on ecosystems and human well-being. *Science*, 355(6332), eaai9214.
949 <https://doi.org/10.1126/science.aai9214>

950 Philippart, C. J. M., Anadón, R., Danovaro, R., Dippner, J. W., Drinkwater, K. F., Hawkins,
951 S. J., Oguz, T., O'Sullivan, G., & Reid, P. C. (2011). Impacts of climate change on
952 European marine ecosystems: Observations, expectations and indicators. *Journal of*
953 *Experimental Marine Biology and Ecology*, 400(1–2), 52–69.
954 <https://doi.org/10.1016/j.jembe.2011.02.023>

955 Pinsky, M. L., Selden, R. L., & Kitchel, Z. J. (2020). Climate-Driven Shifts in Marine Species
956 Ranges: Scaling from Organisms to Communities. *Annual Review of Marine Science*,
957 12(1), 153–179. <https://doi.org/10.1146/annurev-marine-010419-010916>

958 Pither, J. (2003). Climate tolerance and interspecific variation in geographic range size.
959 *Proceedings of the Royal Society of London. Series B: Biological Sciences*, 270(1514),
960 475–481. <https://doi.org/10.1098/rspb.2002.2275>

961 Poloczanska, E. S., Burrows, M. T., Brown, C. J., García Molinos, J., Halpern, B. S., Hoegh-
962 Guldborg, O., Kappel, C. V., Moore, P. J., Richardson, A. J., Schoeman, D. S., &
963 Sydeman, W. J. (2016). Responses of Marine Organisms to Climate Change across
964 Oceans. *Frontiers in Marine Science*, 3. <https://doi.org/10.3389/fmars.2016.00062>

965 Poloczanska, E. S., Brown, C. J., Sydeman, W. J., Kiessling, W., Schoeman, D. S., Moore, P.
966 J., Brander, K., Bruno, J. F., Buckley, L. B., Burrows, M. T., Duarte, C. M., Halpern, B.

967 S., Holding, J., Kappel, C. V., O'Connor, M. I., Pandolfi, J. M., Parmesan, C., Schwing,
968 F., Thompson, S. A., & Richardson, A. J. (2013). Global imprint of climate change on
969 marine life. *Nature Climate Change*, 3(10), 919–925.
970 <https://doi.org/10.1038/nclimate1958>

971 Reiss, H., Cunze, S., König, K., Neumann, H., & Kröncke, I. (2011). Species distribution
972 modelling of marine benthos: A North Sea case study. *Marine Ecology Progress Series*,
973 442, 71–86.

974 R Core Team. (2019). *R: A Language and Environment for Statistical Computing*. Vienna,
975 Austria. Retrieved from <https://www.R-project.org/>

976 Richter, R. (1927). ‘Sandkorallen’—Riffe in der Nordsee. *Natur und Museum*, 57(2), 49–62.

977 Rocchini, D., Hortal, J., Lengyel, S., Lobo, J. M., Jimenez-Valverde, A., Ricotta, C., Bacaro,
978 G., & Chiarucci, A. (2011). Accounting for uncertainty when mapping species
979 distributions: The need for maps of ignorance. *Progress in Physical Geography*, 35(2),
980 211–226.

981 Salomon, J.-C., & Breton, M. (1993). An atlas of long-term currents in the Channel.
982 *Oceanologica Acta*, 16(5), 439–448.

983 Schindler, S., von Wehrden, H., Poirazidis, K., Wrבka, T., & Kati, V. (2013). Multiscale
984 performance of landscape metrics as indicators of species richness of plants, insects and
985 vertebrates. *Linking Landscape Structure and Biodiversity*, 31, 41–48.
986 <https://doi.org/10.1016/j.ecolind.2012.04.012>

987 Schmitt, S., Pouteau, R., Justeau, D., Boissieu, F., & Birnbaum, P. (2017). SSDM: An R
988 package to predict distribution of species richness and composition based on stacked
989 species distribution models. *Methods in Ecology and Evolution*, 8(12), 1795–1803.
990 <https://doi.org/10.1111/2041-210X.12841>

991 Seabra, R., Varela, R., Santos, A. M., Gómez-Gesteira, M., Meneghesso, C., Wethey, D. S., &
992 Lima, F. P. (2019). Reduced Nearshore Warming Associated With Eastern Boundary
993 Upwelling Systems. *Frontiers in Marine Science*, 6, 104.
994 <https://doi.org/10.3389/fmars.2019.00104>

995 Sillero, N., & Barbosa, A. M. (2021). Common mistakes in ecological niche models.
996 *International Journal of Geographical Information Science*, 35(2), 213–226.
997 <https://doi.org/10.1080/13658816.2020.1798968>

998 Steen, V. A., Tingley, M. W., Paton, P. W., & Elphick, C. S. (2021). Spatial thinning and
999 class balancing: Key choices lead to variation in the performance of species distribution
1000 models with citizen science data. *Methods in Ecology and Evolution*, 12(2), 216–226.

1001 Somero, G. (2010). The physiology of climate change: How potentials for acclimatization and
1002 genetic adaptation will determine ‘winners’ and ‘losers’. *Journal of Experimental*
1003 *Biology*, 213(6), 912–920.

1004 Sunday, J. M., Bates, A. E., & Dulvy, N. K. (2012). Thermal tolerance and the global
1005 redistribution of animals. *Nature Climate Change*, 2(9), 686–690.

1006 Thomas, C. D. (2010). Climate, climate change and range boundaries: Climate and range
1007 boundaries. *Diversity and Distributions*, 16(3), 488–495. [https://doi.org/10.1111/j.1472-](https://doi.org/10.1111/j.1472-4642.2010.00642.x)
1008 [4642.2010.00642.x](https://doi.org/10.1111/j.1472-4642.2010.00642.x)

1009 Thuiller, W. (2004). Patterns and uncertainties of species’ range shifts under climate change.
1010 *Global Change Biology*, 10(12), 2020–2027.

1011 Thuiller, W., Lafourcade, B., Engler, R., & Araújo, M. B. (2009). BIOMOD—a platform for
1012 ensemble forecasting of species distributions. *Ecography*, 32(3), 369–373.

1013 Tolman, H. L. (2009). User manual and system documentation of WAVEWATCH III TM
1014 version 3.14. *Technical Note, MMAB Contribution*, 276, 220.

1015 Turner, M. G. (2005). Landscape Ecology: What is the State of the Science? *Annual Review*
1016 *of Ecology, Evolution, and Systematics*, 36, 319–344.
1017 <http://www.jstor.org/stable/30033807>

1018 Tyberghein, L., Verbruggen, H., Pauly, K., Troupin, C., Mineur, F., & De Clerck, O. (2012).
1019 Bio-ORACLE: A global environmental dataset for marine species distribution
1020 modelling: Bio-ORACLE marine environmental data rasters. *Global Ecology and*
1021 *Biogeography*, 21(2), 272–281. <https://doi.org/10.1111/j.1466-8238.2011.00656.x>

1022 Uuemaa, E., Mander, Ü., & Marja, R. (2013). Trends in the use of landscape spatial metrics as
1023 landscape indicators: A review. *10 Years Ecological Indicators*, 28, 100–106.
1024 <https://doi.org/10.1016/j.ecolind.2012.07.018>

1025 VanDerWal, J., Murphy, H. T., Kutt, A. S., Perkins, G. C., Bateman, B. L., Perry, J. J., &
1026 Reside, A. E. (2013). Focus on poleward shifts in species' distribution underestimates
1027 the fingerprint of climate change. *Nature Climate Change*, 3(3), 239–243.
1028 <https://doi.org/10.1038/nclimate1688>

1029 Wallingford, P. D., Morelli, T. L., Allen, J. M., Beaury, E. M., Blumenthal, D. M., Bradley,
1030 B. A., Dukes, J. S., Early, R., Fusco, E. J., Goldberg, D. E., Ibáñez, I., Laginhas, B. B.,
1031 Vilà, M., & Sorte, C. J. B. (2020). Adjusting the lens of invasion biology to focus on the
1032 impacts of climate-driven range shifts. *Nature Climate Change*.
1033 <https://doi.org/10.1038/s41558-020-0768-2>

1034 Walther, G.-R. (2010). Community and ecosystem responses to recent climate change.
1035 *Philosophical Transactions of the Royal Society B: Biological Sciences*, 365(1549),
1036 2019–2024. <https://doi.org/10.1098/rstb.2010.0021>

1037 Wenger, S. J., & Olden, J. D. (2012). Assessing transferability of ecological models: An
1038 underappreciated aspect of statistical validation. *Methods in Ecology and Evolution*,
1039 3(2), 260–267.

1040 Wethey, D. S., Woodin, S. A., Hilbish, T. J., Jones, S. J., Lima, F. P., & Brannock, P. M.
1041 (2011). Response of intertidal populations to climate: Effects of extreme events versus
1042 long term change. *Journal of Experimental Marine Biology and Ecology*, 400(1–2),
1043 132–144. <https://doi.org/10.1016/j.jembe.2011.02.008>

1044 Wilson, D. P. (1971). Sabellaria Colonies At Duckpool, North Cornwall, 1961–1970. *Journal*
1045 *of the Marine Biological Association of the United Kingdom*, 51(03), 509.
1046 <https://doi.org/10.1017/S002531540001496X>

1047 Wort, E. J., Chapman, M. A., Hawkins, S. J., Henshall, L., Pita, A., Rius, M., Williams, S. T.,
1048 & Fenberg, P. B. (2019). Contrasting genetic structure of sympatric congeneric
1049 gastropods: Do differences in habitat preference, abundance and distribution matter?
1050 *Journal of Biogeography*, 46(2), 369–380.

1051 Wright, J. P. (2009). Linking populations to landscapes: Richness scenarios resulting from
1052 changes in the dynamics of an ecosystem engineer. *Ecology*, 90(12), 3418–3429.

1053 Yalcin, S., & Leroux, S. J. (2017). Diversity and suitability of existing methods and metrics
1054 for quantifying species range shifts. *Global Ecology and Biogeography*, 26(6), 609–624.

1055 Yates, K. L., Bouchet, P. J., Caley, M. J., Mengersen, K., Randin, C. F., Parnell, S., Fielding,
1056 A. H., Bamford, A. J., Ban, S., & Barbosa, A. M. (2018). Outstanding challenges in the
1057 transferability of ecological models. *Trends in Ecology & Evolution*, 33(10), 790–802.

1058